JOURNAL OF APPLIED CRYSTALLOGRAPHY

Volume 53 (2020)

Supporting information for article:

Instrument-model refinement in normalised reciprocal-vector space for X-ray Laue diffraction

Radoslaw Kaminski, Dariusz Szarejko, Martin N. Pedersen, Lauren E. Hatcher, Piotr Laski, Paul R. Raithby, Michael Wulff and Katarzyna N. Jarzembska

Instrument-model refinement in normalised reciprocal-vector space for X-ray Laue diffraction

Radosław Kamiński,[a,*] Dariusz Szarejko,[a] Martin N. Pedersen,[b] Lauren E. Hatcher,[c,d] Piotr Łaski,[a] Paul R. Raithby,[c] Michael Wulff,[e] Katarzyna N. Jarzembska [a,*]

[a] Department of Chemistry, University of Warsaw, Żwirki i Wigury 101, 02-089 Warsaw, Poland

[b] Niels Bohr Institute, University of Copenhagen, Universitetsparken 5, 2100 Copenhagen, Denmark

[c] Department of Chemistry, University of Bath, Claverton Down, Bath, BA2 7AY, United Kingdom

[d] School of Chemistry, Cardiff University, Main Building, Park Place, Cardiff, CF10 3AT, United Kingdom

[e] European Synchrotron Radiation Facility, 71 avenue des Martyrs, 38043 Grenoble, France

* Corresponding authors: Radosław Kamiński (rkaminski85@uw.edu.pl)
Katarzyna N. Jarzembska (katarzyna.jarzembska@uw.edu.pl)

S1. Instrument model and refinement details

Matrix notation for vectors is used; $\mathbf{a}^{\mathrm{T}}$ stands for a transpose of the matrix $\mathbf{a}$; scalar product in Cartesian basis is $\mathbf{a} \cdot \mathbf{b} = \mathbf{a}^{\mathrm{T}}\mathbf{b}$; for clarity in the text column vectors are written as rows, *i.e.* $[a_1 \quad a_2 \quad \ldots]^{\mathrm{T}}$. When needed the coordinate system is added in the subscript (*i.e.* $[\cdot]_S$ is matrix of vector components in coordinate system S). Laboratory coordinate system $L = (\mathbf{e}_x, \mathbf{e}_y, \mathbf{e}_z)$ is placed in the ideal goniometer centre (X axis along X-ray beam, Z vertical to the top). Primary X-ray beam position is assumed to be fixed along the X axis (*i.e.* along the $\mathbf{e}_x$ vector): $\mathbf{s}_0 = \mathbf{e}_x = [1 \quad 0 \quad 0]^{\mathrm{T}}_L$. Detector coordinate system $D_0 = (\mathbf{d}_x, \mathbf{d}_y, \mathbf{d}_z)$ is anchored in the detector centre (X axis horizontal, Y vertical). Spot position expressed in D_0 is described as vector $\mathbf{r} = [x \quad y \quad 0]^{\mathrm{T}}_{D_0}$, whereas the position of the point where the primary beam hits the detector is $\mathbf{r}_0 = [x_0 \quad y_0 \quad 0]^{\mathrm{T}}_{D_0}$. Position of the spot in respect to the primary beam position is $\Delta\mathbf{r} = \mathbf{r} - \mathbf{r}_0 = [x - x_0 \quad y - y_0 \quad 0]^{\mathrm{T}}_{D_0}$. Calculation of normalised $\underset{\sim}{\mathbf{h}}$ in L is obtained by the following formulas:

$$\mathbf{x} = d \cdot \mathbf{s}_0 + \Delta\mathbf{r} = \begin{bmatrix} d \\ -(x - x_0) \\ y - y_0 \end{bmatrix}_L \tag{S1}$$

$$\mathbf{s} = \frac{\mathbf{x}}{\|\mathbf{x}\|} \quad , \quad \mathbf{y} = \mathbf{s} - \mathbf{s}_0 \quad , \quad \underset{\sim}{\mathbf{h}} = \frac{\mathbf{y}}{\|\mathbf{y}\|} \tag{S2}$$

where $\|\cdot\|$ is the vector norm. See Figure 1S for visualisation of respective vectors and coordinate systems. Finally, vector $\underset{\sim}{\mathbf{h}}$ rotated to the goniometer-head-fixed coordinate system $G = (\mathbf{g}_x, \mathbf{g}_y, \mathbf{g}_z)$ is obtained by application of the rotation matrix $\mathbf{R}$, different for each frame: $\underset{\sim}{\mathbf{h}}_0 = \mathbf{R}^{\mathrm{T}}\underset{\sim}{\mathbf{h}}$ (where $\mathbf{R}^{-1} = \mathbf{R}^{\mathrm{T}}$). Note that G and L coordinate systems overlay for all goniometer angles set to zero.

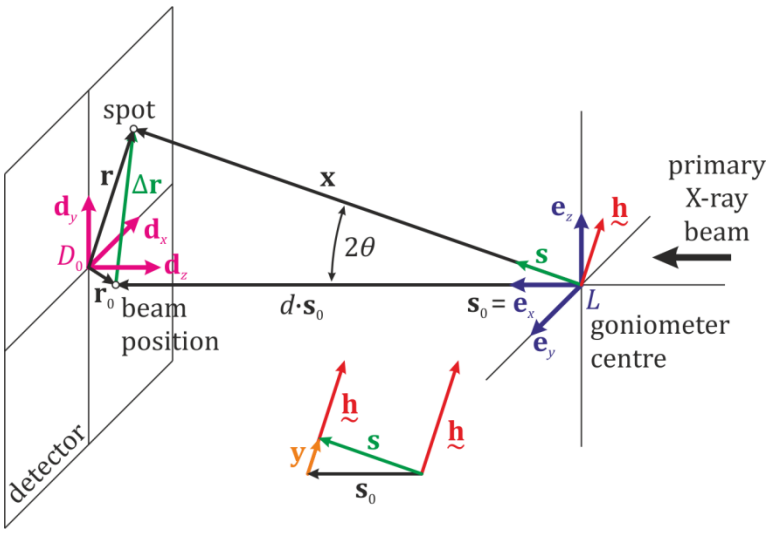

Figure S1 Detector and laboratory coordinate systems, $D_0 = (\mathbf{d}_x, \mathbf{d}_y, \mathbf{d}_z)$ and $L = (\mathbf{e}_x, \mathbf{e}_y, \mathbf{e}_z)$, and vectors needed in the calculations.

Native ('raw') spot position on the detector is expressed in $D_2 = (\mathbf{i}, \mathbf{j}, \mathbf{k})$ pixel-based coordinate system anchored in the centre of the top left detector pixel (right-handed, $\mathbf{i}$ points down, $\mathbf{j}$ right); this is a basic definition used in majority of image processing applications. We introduce real-valued coordinate system $D_1 = (\boldsymbol{\delta}_x, \boldsymbol{\delta}_y, \boldsymbol{\delta}_z)$ centred on top left detector corner (orientation the same as for D_2). Relations of spot coordinates in D_0 and these two coordinate systems are expressed by the following formulas:

$$\begin{bmatrix} x \\ y \\ 0 \end{bmatrix}_{D_0} = \begin{bmatrix} x_\delta - \frac{1}{2}p_\mathrm{h}n_\mathrm{h} \\ \frac{1}{2}p_\mathrm{v}n_\mathrm{v} - y_\delta \\ 0 \end{bmatrix}_{D_1} = \begin{bmatrix} j + \frac{1}{2}p_\mathrm{h}(1 - n_\mathrm{h}) \\ \frac{1}{2}p_\mathrm{v}(n_\mathrm{v} - 1) - i \\ 0 \end{bmatrix}_{D_2} \tag{S3}$$

where n_h and n_v are number of detector pixels, and p_h and p_v are pixel sizes, for horizontal and vertical directions, respectively.

To perform a least-squares minimisation the derivatives of the norm of the difference of two computed $\underset{\sim}{\mathbf{h}}_0$ vectors for the same spot appearing for two consecutive frames (*i.e.* $\Delta\underset{\sim}{\mathbf{h}}_{0,k,j} = \underset{\sim}{\mathbf{h}}_{0,k,j} - \underset{\sim}{\mathbf{h}}_{0,k,j+1}$) are needed. The derivatives are computed as follows:

$$\frac{\partial}{\partial p}\left\|\Delta\underset{\sim}{\mathbf{h}}_{0,k,j}\right\| = \frac{\Delta\underset{\sim}{\mathbf{h}}_{0,k,j}^{T}}{\left\|\Delta\underset{\sim}{\mathbf{h}}_{0,k,j}\right\|}\left(\frac{\partial}{\partial p}\underset{\sim}{\mathbf{h}}_{0,k,j} - \frac{\partial}{\partial p}\underset{\sim}{\mathbf{h}}_{0,k,j+1}\right) \tag{S4}$$

where $\underset{\sim}{\mathbf{h}}_{0,k,j}$ is vector for the k-pair of $\underset{\sim}{\mathbf{h}}_0$ vectors matched for frames j and $j+1$; p is selected refined parameter. Accordingly (for clarity we drop indexes k and j; note matrices $\mathbf{R}$ depend on frame index j):

$$\frac{\partial}{\partial p}\underset{\sim}{\mathbf{h}}_0 = \mathbf{R}^{\mathrm{T}}\left(\frac{1}{\|\mathbf{y}\|}\left(\frac{\partial\mathbf{y}}{\partial p}\right) - \frac{\mathbf{y}}{\|\mathbf{y}\|^3}\left[\mathbf{y}^{\mathrm{T}}\left(\frac{\partial\mathbf{y}}{\partial p}\right)\right]\right) \tag{S5}$$

$$\frac{\partial\mathbf{y}}{\partial p} = \frac{1}{\|\mathbf{x}\|}\left(\frac{\partial\mathbf{x}}{\partial p}\right) - \frac{\mathbf{x}}{\|\mathbf{x}\|^3}\left[\mathbf{x}^{\mathrm{T}}\left(\frac{\partial\mathbf{x}}{\partial p}\right)\right] \tag{S6}$$

Since $\mathbf{x} = [d \quad -(x-x_0) \quad y-y_0]_L^{\mathrm{T}}$ its derivatives simply equal to:

$$\frac{\partial\mathbf{x}}{\partial d} = \begin{bmatrix}1\\0\\0\end{bmatrix}_L \quad , \quad \frac{\partial\mathbf{x}}{\partial x_0} = \begin{bmatrix}0\\1\\0\end{bmatrix}_L \quad , \quad \frac{\partial\mathbf{x}}{\partial y_0} = \begin{bmatrix}0\\0\\-1\end{bmatrix}_L \tag{S7}$$

Please note the actual implementation of the procedure works in native detector pixel coordinates, as denoted above in the equation S3. Therefore, inside the program source code the last component of the third derivative in S7 (*i.e.* $\partial\mathbf{x}/\partial y_0$) is in fact positive.

Reflections from two consecutive frames j and $j+1$ are considered to form a pair k when the simple geometrical criterion,

$$\arccos\left(\underset{\sim}{\mathbf{h}}_{0,k,j}^{\mathrm{T}}\underset{\sim}{\mathbf{h}}_{0,k,j+1}\right) = \theta \le \theta_0 \tag{S8}$$

is fulfilled, where θ_0 is the specified threshold (note here both vectors are of unit length, thus obviously $\left\|\underset{\sim}{\mathbf{h}}_{0,k,j}\right\| \cdot \left\|\underset{\sim}{\mathbf{h}}_{0,k,j+1}\right\| = 1$).

S2. Simulation of X-ray Laue patterns

Instrument model used in simulations is more general, which provides more flexibility for future applications. In addition to coordinate systems L and G, presented in the previous section, we define also extra coordinate systems $K^* = (\mathbf{a}^*, \mathbf{b}^*, \mathbf{c}^*)$ (non-Cartesian reciprocal crystal coordinate system) and $C = (\mathbf{c}_x, \mathbf{c}_y, \mathbf{c}_z)$ (introduced to easily decompose the orientation matrix into 'orientation' and 'unit-cell shape' parts). The transformation between K^* and C systems is defined with the following matrix $\mathbf{B}$ (expressed in reciprocal lattice unit cell parameters):

$$\mathbf{B} = \begin{bmatrix} a^* & 0 & 0 \\ b^*\cos(\gamma^*) & b^*\sin(\gamma^*) & 0 \\ c^*\cos(\beta^*) & c^*\dfrac{\cos(\alpha^*)-\cos(\gamma^*)\cos(\beta^*)}{\sin(\gamma^*)} & c^*\left[1-\cos(\beta^*)-\dfrac{\cos(\alpha^*)-\cos(\gamma^*)\cos(\beta^*)}{\sin(\gamma^*)}\right] \end{bmatrix} \tag{S9}$$

where the transformation takes the form:

$$\mathbf{h}_C = \mathbf{B}^{\mathrm{T}} \cdot \mathbf{h}_{K^*} \tag{S10}$$

in which $\mathbf{h} = h\mathbf{a}^* + k\mathbf{b}^* + l\mathbf{c}^* = x_{\mathrm{c}}\mathbf{c}_x + y_{\mathrm{c}}\mathbf{c}_y + z_{\mathrm{c}}\mathbf{c}_z$. The relationship between K^* and C frames is depicted in Figure 2S.

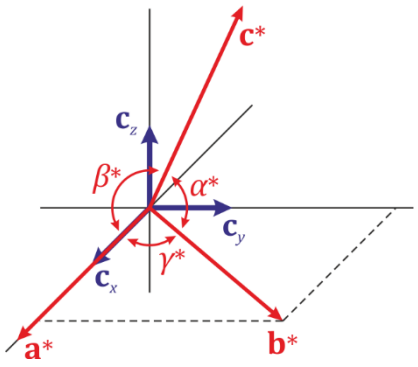

Figure S2 Relationship between $C = (\mathbf{c}_x, \mathbf{c}_y, \mathbf{c}_z)$ and $K^* = (\mathbf{a}^*, \mathbf{b}^*, \mathbf{c}^*)$ coordinate systems. Vector $\mathbf{a}^*$ is along $\mathbf{c}_x$, and $\mathbf{b}^*$ lies in the plane formed by $\mathbf{c}_x$ and $\mathbf{c}_y$ vectors.

For computational purposes the matrix **B** is expressed in direct lattice unit-cell parameters using the very well-known formulas:

$$a^* = \frac{bc\sin\alpha}{V} \qquad b^* = \frac{ac\sin\beta}{V} \qquad c^* = \frac{ab\sin\gamma}{V}$$

$$\cos(\alpha^*) = \frac{\cos\beta\cos\gamma - \cos\alpha}{\sin\beta\sin\gamma} \qquad \cos(\beta^*) = \frac{\cos\alpha\cos\gamma - \cos\beta}{\sin\alpha\sin\gamma} \qquad \cos(\gamma^*) = \frac{\cos\alpha\cos\beta - \cos\gamma}{\sin\alpha\sin\beta} \tag{S11}$$

$$\sin(\gamma^*) = \frac{V}{abc\sin\alpha\sin\beta} \qquad V = abc\sqrt{1-\cos^2\alpha-\cos^2\beta-\cos^2\gamma+2\cos\alpha\cos\beta\cos\gamma}$$

Orientation matrix **U** describes how the crystal reciprocal axes are related to the goniometer-head-fixed coordinate system (*i.e.* relation between K^* and G coordinate systems). We define the matrix **U** as follows:

$$\mathbf{h}_G = \mathbf{U} \cdot \mathbf{h}_{K^*} \tag{S12}$$

where for any vector we have $\mathbf{h} = h\mathbf{a}^* + k\mathbf{b}^* + l\mathbf{c}^* = x_{\mathrm{g}}\mathbf{g}_x + y_{\mathrm{g}}\mathbf{g}_y + z_{\mathrm{g}}\mathbf{g}_z$. This definition is identical to the one used by Kalinowski *et al.* (Kalinowski *et al.*, 2011) and closely related to the definitions used in the seminal paper by Busing & Levy (Busing & Levy, 1967). The relation between G and C coordinate systems (both are Cartesian) is then expressed with matrix **C** as follows:

$$\mathbf{h}_G = \mathbf{C}^{\mathrm{T}} \cdot \mathbf{h}_C \tag{S13}$$

From this definition it follows that $\mathbf{h}_G = \mathbf{C}^{\mathrm{T}}\mathbf{B}^{\mathrm{T}} \cdot \mathbf{h}_{K^*} = (\mathbf{BC})^{\mathrm{T}} \cdot \mathbf{h}_{K^*}$. Rotation matrix $\mathbf{C}$ is expressed via Euler angles (θ_1, θ_2 and θ_3) in the following way:

$$\mathbf{C} = \mathbf{R}_1(\theta_1) \cdot \mathbf{R}_2(\theta_2) \cdot \mathbf{R}_3(\theta_3) \tag{S14}$$

where

$$\mathbf{R}_1(\theta_1) = \begin{bmatrix} \cos(\theta_1) & -\sin(\theta_1) & 0 \\ \sin(\theta_1) & \cos(\theta_1) & 0 \\ 0 & 0 & 1 \end{bmatrix} \quad \mathbf{R}_2(\theta_2) = \begin{bmatrix} 1 & 0 & 0 \\ 0 & \cos(\theta_2) & -\sin(\theta_2) \\ 0 & \sin(\theta_2) & \cos(\theta_2) \end{bmatrix} \quad \mathbf{R}_3(\theta_3) = \begin{bmatrix} \cos(\theta_3) & -\sin(\theta_3) & 0 \\ \sin(\theta_3) & \cos(\theta_3) & 0 \\ 0 & 0 & 1 \end{bmatrix} \tag{S15}$$

Finally, every crystal is appropriately rotated on the goniometer. We assume all rotations of the goniometer are defined as counter-clockwise. When the goniometer angles are rotated, the selected **h** vector is rotated alongside with the goniometer-head-fixed coordinate system G (*i.e.* vector **h** coordinates in G remain constant). General scheme of the Euler-type goniometer is presented in Figure 3S. We introduce two other Cartesian coordinate systems associated with ω and χ circles: $O = (\mathbf{o}_x, \mathbf{o}_y, \mathbf{o}_z)$ and $M = (\mathbf{m}_x, \mathbf{m}_y, \mathbf{m}_z)$. We note when all seting angles are zero the G, O and M coordinate systems overlay with L. We now systematically define all counter-clockwise rotations along ω, χ and ϕ axes (the same symbols are used for respective angles) as:

$$\mathbf{h}_L = \mathbf{R}_z(\omega) \cdot \mathbf{h}_O \tag{S16}$$

$$\mathbf{h}_O = \mathbf{R}_x(\chi) \cdot \mathbf{h}_M \tag{S17}$$

$$\mathbf{h}_M = \mathbf{R}_z(\phi) \cdot \mathbf{h}_G \tag{S18}$$

This, finally, yields a total rotation as:

$$\mathbf{h}_L = \mathbf{R} \cdot \mathbf{h}_G \tag{S19}$$

where the matrix **R** takes the form:

$$\mathbf{R} = \mathbf{R}_z(\omega) \cdot \mathbf{R}_x(\chi) \cdot \mathbf{R}_z(\phi) \tag{S20}$$

and

$$\mathbf{R}_z(\omega) = \begin{bmatrix} \cos\omega & -\sin\omega & 0 \\ \sin\omega & \cos\omega & 0 \\ 0 & 0 & 1 \end{bmatrix} \quad \mathbf{R}_x(\chi) = \begin{bmatrix} 1 & 0 & 0 \\ 0 & \cos\chi & -\sin\chi \\ 0 & \sin\chi & \cos\chi \end{bmatrix} \quad \mathbf{R}_z(\phi) = \begin{bmatrix} \cos\phi & -\sin\phi & 0 \\ \sin\phi & \cos\phi & 0 \\ 0 & 0 & 1 \end{bmatrix} \tag{S21}$$

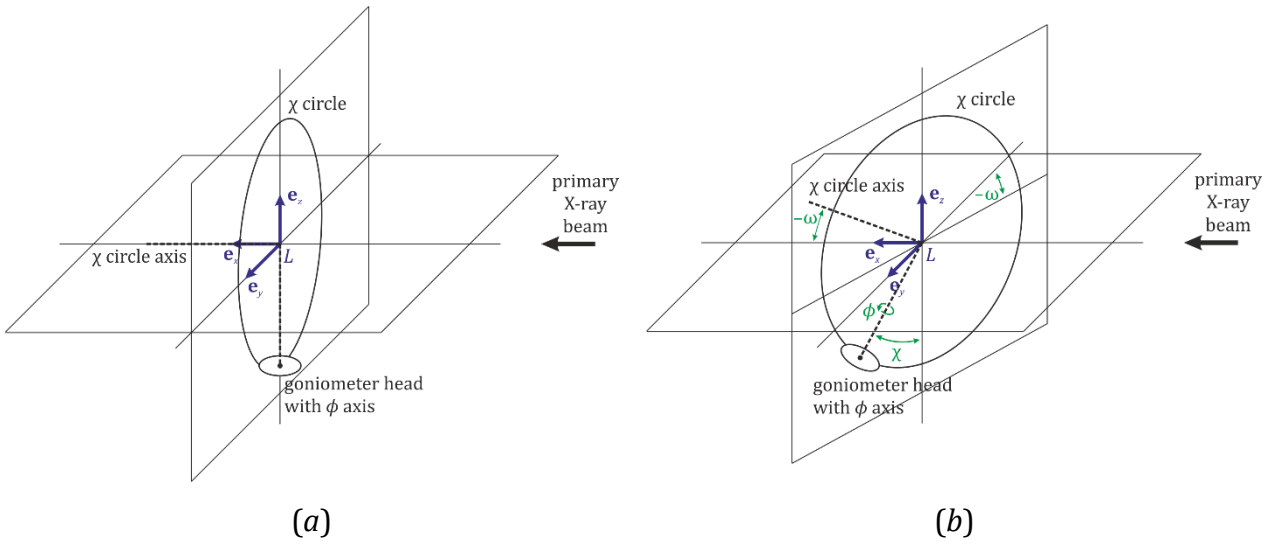

Figure S3 Schematic representation of the 4-circle Euler-type goniometer. (*a*) The instrument with all angles set to zero. (*b*) Instrument with all angles departed from zero position (all rotations are defined as positive then counter-clockwise; for clarity of the figure the ω is shown as negative).

Finally, the equation allowing to compute the coordinates of vector $\mathbf{h}$ in laboratory frame L given all the matrices and transformation is as follows:

$$\mathbf{h}_L = \mathbf{R} \cdot \mathbf{h}_G = \mathbf{R} \cdot (\mathbf{BC})^{\mathrm{T}} \cdot \mathbf{h}_{K^*} \tag{S22}$$

Where we introduced vector $\mathbf{h}_0 = \mathbf{h}_G = (\mathbf{BC})^{\mathrm{T}}\mathbf{h}_{K^*}$ (*i.e.* vector $\mathbf{h}$ before goniometer rotation angles applied, as in the previous section; notation $\mathbf{h}_0$ is used in the main text for convenience).

For Laue diffraction every spot falling into the region between two extreme Ewald spheres is recorded. For each $\mathbf{h}$ vector its wavelength is calculated using a well-known formula:

$$\lambda = -2\frac{\mathbf{h} \cdot \mathbf{s}_0}{\|\mathbf{h}\|^2} = -2\frac{\mathbf{h} \cdot \mathbf{s}_0}{\mathbf{h} \cdot \mathbf{h}} \tag{S23}$$

The implemented algorithm follows then a simple path:

(i) Generation of the allowed $\mathbf{h}_{K^*}$ vector indices (*i.e.* h, k and l) in reciprocal crystal basis K^*. Limiting values are estimated from the larger Ewald sphere radius ($1/\lambda_{\mathrm{min}}$). Additional $\sin\theta\,/\lambda$ cut-off can be taken into account. At this point the systematic absences can also omitted (not implemented yet).

(ii) Generated $\mathbf{h}_{K^*}$ vectors are transformed to the goniometer-head-fixed Cartesian reference frame of G using the $\mathbf{h}_G = (\mathbf{BC})^{\mathrm{T}}\mathbf{h}_{K^*}$. This set is used in the next steps.

(iii) For every frame (with known frame rotation angles) all $\mathbf{h}_G$ are rotated to the laboratory frame L: $\mathbf{h}_L = \mathbf{R} \cdot \mathbf{h}_0$.

(iv) For each $\mathbf{h}_L$ the wavelength at which the diffraction would occur for this particular vector is computed. At this step we check whether the computed values falls into the region between two limiting Ewald spheres, *i.e.* if $\lambda_{\min} \leq \lambda \leq \lambda_{\max}$. If this is fulfilled the algorithm proceeds further, otherwise the vector is rejected.

(v) Diffraction equation is used to compute the scattering vector $\mathbf{s} = \mathbf{s}_0 + \lambda \cdot \mathbf{h}_L$, and it is checked whether the detector surface intersects the line along this vector (i.e. we check if the spot lies in the detector area). If the last is true, the coordinates of the spot on the detector are computed and saved into the HDF5 file.

(vi) Steps (iii)-(v) are repeated for all frames (a number specified by the user).

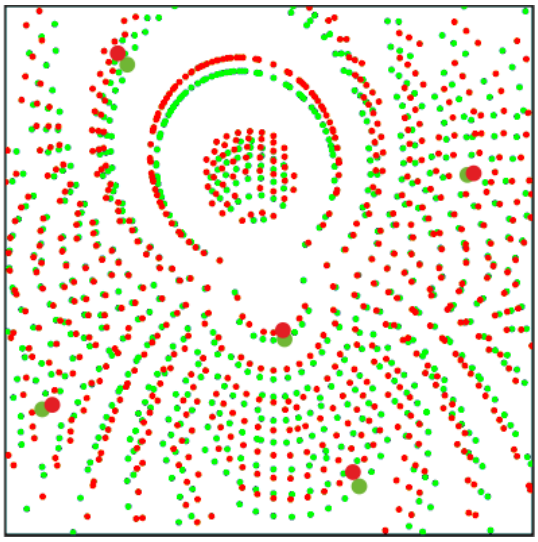

Figure S4 Overlay of two adjacent frames (angular interval $\Delta\phi$ = 1°) shown for simulated data (silver(I)-copper(I) complex quoted in the main text) – green spots: frame for ϕ = 0°, red spots: frame for ϕ = 1° (crystal horizontal rotation). Large dots represent selected reflections shown in Figure 1*b*.

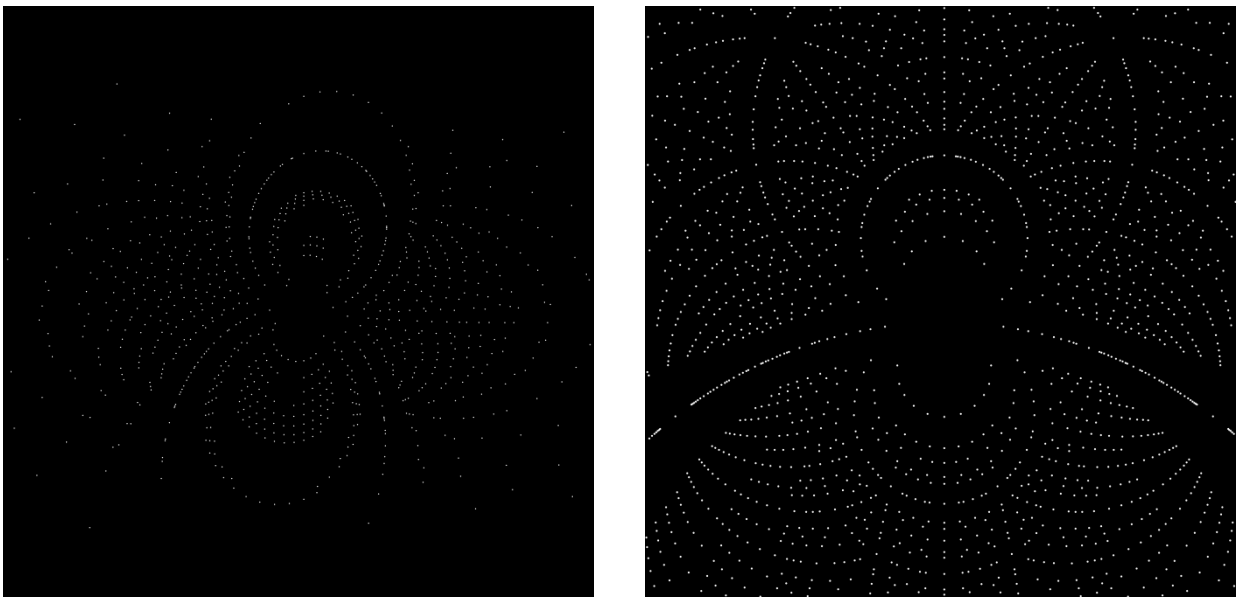

(*a*) (*b*)

Figure S5 Example simulated frames. (*a*) Single frame generated for the **simAgCu** test sample. (*b*) Single frame generated for the **simPeaL** test sample. For simulation details see Table 1 in the manuscript text.

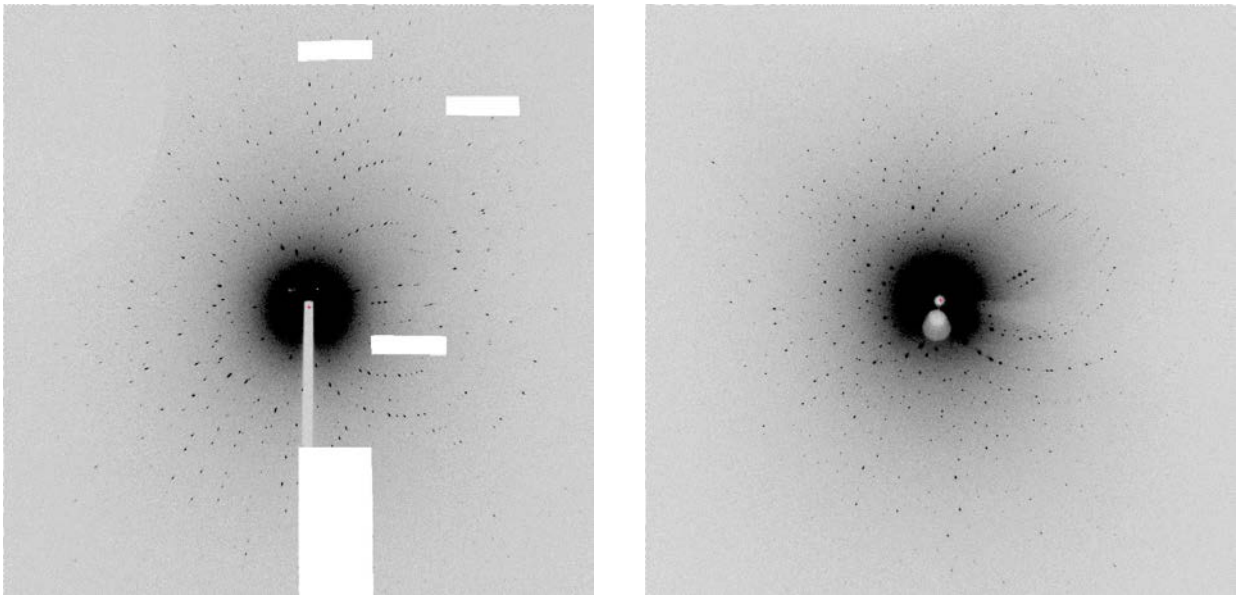

(*a*) (*b*)

Figure S6 Example experimental frames. (*a*) Single frame recorded at the 14-ID-B beamline at APS for the **expCuDppe** sample (15 keV 'pink' X-ray beam, detector: Rayonix MX340-HS, detector distance: 100 mm, note some unusable detector areas not used in processing). (*b*) Single frame recorded at the ID09 beamline at ESRF for the **expCuDmdpp** sample (15 keV 'pink' X-ray beam, detector: Rayonix MX170-HS, detector distance: 50 mm, note two beamstops are present: the top one – smaller and closer to the detector centre – is for X-rays, and bottom is for the laser beam used in TR experiments).